

## Accepted Manuscript

Discovery and structure-based design of 4,6-diaminonicotinamides as potent and selective IRAK4 inhibitors

Rajeev S. Bhide, Alec Keon, Carolyn Weigelt, John S. Sack, Robert J. Schmidt, Shuqun Lin, Hai-Yun Xiao, Steven H. Spergel, James Kempson, William J. Pitts, Julie Carman, Michael A. Poss

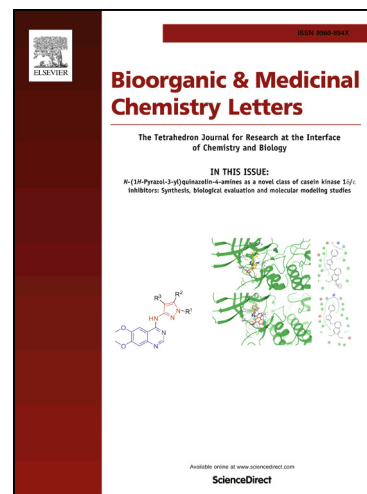
PII: S0960-894X(17)30925-3  
DOI: <http://dx.doi.org/10.1016/j.bmcl.2017.09.029>  
Reference: BMCL 25293

To appear in: *Bioorganic & Medicinal Chemistry Letters*

Received Date: 12 May 2017  
Revised Date: 12 September 2017  
Accepted Date: 13 September 2017

Please cite this article as: Bhide, R.S., Keon, A., Weigelt, C., Sack, J.S., Schmidt, R.J., Lin, S., Xiao, H-Y., Spergel, S.H., Kempson, J., Pitts, W.J., Carman, J., Poss, M.A., Discovery and structure-based design of 4,6-diaminonicotinamides as potent and selective IRAK4 inhibitors, *Bioorganic & Medicinal Chemistry Letters* (2017), doi: <http://dx.doi.org/10.1016/j.bmcl.2017.09.029>

This is a PDF file of an unedited manuscript that has been accepted for publication. As a service to our customers we are providing this early version of the manuscript. The manuscript will undergo copyediting, typesetting, and review of the resulting proof before it is published in its final form. Please note that during the production process errors may be discovered which could affect the content, and all legal disclaimers that apply to the journal pertain.





## Discovery and structure-based design of 4,6-diaminonicotinamides as potent and selective IRAK4 inhibitors

Rajeev S. Bhide<sup>\* a</sup>, Alec Keon<sup>a</sup>, Carolyn Weigelt<sup>b</sup>, John S. Sack<sup>b</sup>, Robert J. Schmidt<sup>a</sup>, Shuqun Lin<sup>a</sup>, Hai-Yun Xiao<sup>a</sup>, Steven H. Spergel<sup>a</sup>, James Kempson, William J. Pitts<sup>a</sup>, Julie Carman<sup>c</sup>, and Michael A. Poss<sup>a</sup>

<sup>a</sup>Discovery Chemistry, Research & Development, Bristol-Myers Squibb Company, Route 206 & Province Line Road, Princeton, NJ 08543

<sup>b</sup>Molecular Structure and Design, Research & Development, Bristol-Myers Squibb Company, Route 206 & Province Line Road, Princeton, NJ 08543

<sup>c</sup>Immunoscience Biology, Research & Development, Bristol-Myers Squibb Company, Route 206 & Province Line Road, Princeton, NJ 08543

### ARTICLE INFO

#### Article history:

Received  
Revised  
Accepted  
Available online

### ABSTRACT

The identification of small molecule inhibitors of IRAK4 for the treatment of autoimmune diseases has been an area of intense research. We discovered novel 4,6-diaminonicotinamides which potently inhibit IRAK4. Optimization efforts were aided by x-ray crystal structures of inhibitors bound to IRAK4. Structure activity relationship (SAR) studies led to the identification of compound **29** which exhibited sub-micromolar potency in a LTA stimulated cellular assay.

#### Keywords:

IRAK4  
4,6-diaminonicotinamide  
Rheumatoid arthritis  
Autoimmune disease

2009 Elsevier Ltd. All rights reserved.

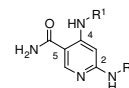
Treatment of autoimmune diseases such as rheumatoid arthritis (RA), inflammatory bowel disease (IBD) and Systemic Lupus Erythematosus (SLE) has been an area of intense research over the past two decades. Various mechanisms that impact innate and/or adaptive immunity have been targeted for the management of these autoimmune disorders.<sup>1</sup>

Interleukin-1 Receptor Associated Kinase 4 (IRAK4) is a serine/threonine kinase that regulates signaling through various TLRs including TLR2, 4, 5, and 7-9 which are involved in the innate immune response.<sup>2</sup> IRAK4 also regulates signaling through members of the IL-1 family, and can therefore impact adaptive immunity as well.<sup>3</sup> Cells from IRAK4 deficient humans fail to respond to agonists of the TLRs described above, and to members of the IL-1 family.<sup>4</sup> These patients are highly susceptible to bacterial infections in childhood, but this risk decreases with age.<sup>5</sup> IRAK4 kinase-dead knock-in mice have shown beneficial effects in mouse models of arthritis<sup>6</sup> and therefore, discovery of small molecule inhibitors of IRAK4 has become an important subject of research.<sup>7,8</sup> Recently, a potent IRAK4 inhibitor, PF-06650833, has entered phase 2 clinical trials (NCT02996500) for the treatment of RA<sup>9</sup> and BAY 1834845 has entered phase 1 clinical trials (NCT03054402).

A review of kinase enzyme inhibition data for compounds from our JAK3 program led to the identification of a set of analogs from a 4,6-nicotinamide series which showed moderate inhibition of IRAK4 (Table 1). Analysis of this modest set of compounds showed that substituents on the aryl group at C2

generally resulted in modest improvements in IRAK4 potency (compare **1** with **4-6** and **8**), with the notable exception of **7** which did not inhibit IRAK4 at the concentrations tested. The ethanolamine substituents (**2**, **3**) at C4 also improved the IRAK4 potency by about 2-fold, with **2** being notable due to its significant decrease in JAK3 potency. However, the SAR was not immediately apparent from these compounds due to changes at both C2 and C4. While the observations discussed above could have formed the basis of a chemistry SAR plan, we chose to first examine JAK3 and IRAK4 inhibitor complexes to better guide our optimization effort.

**Table 1.** IRAK4 hit identification.



Compound	R <sup>1</sup>	R <sup>2</sup>	IRAK4 <sup>a</sup> IC <sub>50</sub> (nM)	JAK3 <sup>a</sup> IC <sub>50</sub> (nM)
1			1800	5
2			730	1000
3			840	8
4			360	3
5			390	9
6			470	7
7			>10000	2
8			180	3

<sup>a</sup>Kinase activity was measured by Caliper assays, minimum in duplicate, average IC<sub>50</sub> reported.<sup>10</sup>

Initially, we were intrigued by extended amide **7**, a potent inhibitor of JAK3 that also displayed high selectivity against IRAK4, and therefore obtained an X-ray co-crystal structure of **7** in JAK3. From the structure, it was noted that the pyridine nitrogen and NH of the CONH<sub>2</sub> group of **7** bind to the hinge region of JAK3 kinase (Figure 1) while the C2 substituent projects out towards solvent.<sup>11</sup> In comparison, IRAK4 has several unique structural features including a loop insertion in the N-terminal region (Shellman loop) which is in close proximity to the ATP binding site.<sup>12</sup> One hypothesis for the poor IRAK4 potency of **7** was the possibility of an unfavorable steric interaction between the bulky C2 substituent of **7** and the Shellman loop region of IRAK4. Given the unique structural features of IRAK4, an alternative hypothesis considered that compounds **1-6**, and **8** might be binding to IRAK4 in a different binding mode.

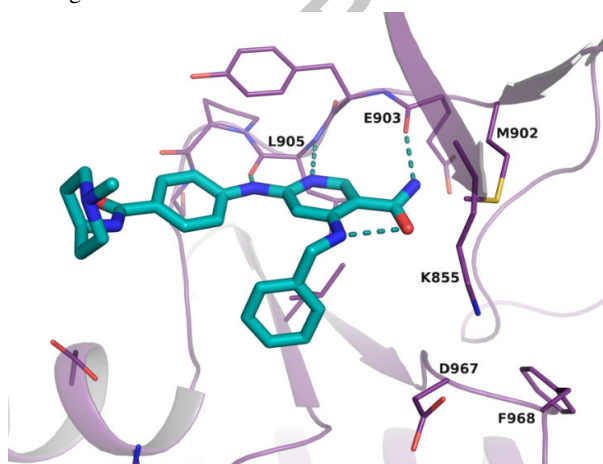


**Figure 1.** Crystal structure of **7** in JAK3 kinase domain. Residues possibly involved in hydrogen bonds are labeled, and bonds are shown by dotted lines. (PDB code 5W86).

Additional structural information was then obtained from an X-ray co-crystal structure of **4** in IRAK4 (Figure 2) which revealed that **4** was bound to IRAK4 in a ‘flipped’ binding mode, compared to the mode observed in the JAK3 crystal structure. In this ‘flipped’ mode, hydrogen bonding interactions between the NH at C2, the pyridyl nitrogen, and the NH of the amide of **4** with the hinge region of IRAK4 form a ‘classical’ triad hinge binding interaction. Another feature of this binding mode is that the C2 substituent of **4** is oriented towards the Tyr262 gatekeeper in an apparent  $\pi$  stacking interaction. We were pleased by this observation as the IRAK family of kinases are the only ones which possess a tyrosine gatekeeper residue. We hoped that by engaging this interaction, improvements in kinome selectivity could be realized. In addition, the C2 substituent of **4** forms a hydrogen bond between the indolone carbonyl and the amine of Lys213. Ligand docking experiments of the compounds in Table 1 into this IRAK4 crystal structure revealed that **7** failed to achieve a suitable pose, presumably due to the inability of the gatekeeper pocket to accommodate the extended amide. In contrast, compounds **1-3**, **5**, **6** and **8** could be docked in a manner similar to **4**. We also noticed that the primary amide group of **4** was oriented towards the solvent exposed region and the Shellman loop, whereas in JAK3, the primary amide was oriented towards the bulky gatekeeper, Met902. Based on these observations, we reasoned that introduction of a substituent on the amide group should further disfavor binding to JAK3, but may be permissible in IRAK4, thereby possibly affording selectivity for IRAK4 against JAK3.

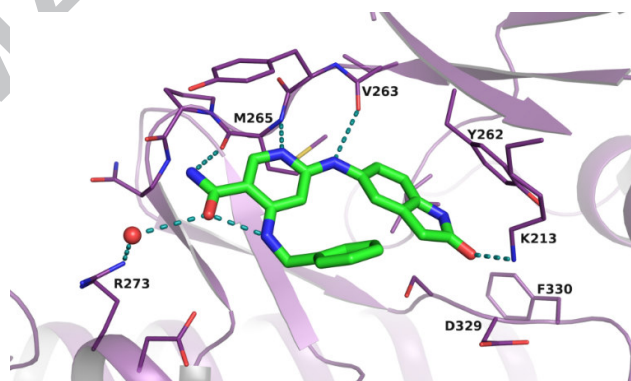
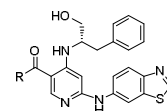


**Figure 2.** Crystal structure of **4** in IRAK4 kinase domain. Residues possibly involved in hydrogen bonds are labeled and bonds are shown by dotted lines. (PDB code 5W84).

To test these assertions, we proceeded to expand the scope of amide substitution at the C5 position. We chose the C4 substituent of **2** in an effort to disfavor JAK3 binding and the C2 substituent of **8**, as that substituent was present in the most potent IRAK4 inhibitor. Compounds were prepared by the route presented in Scheme 1, with minor variations.<sup>10</sup>

**Table 2.** SAR at C5 amide.



Compound	R	IRAK4 <sup>a</sup> IC <sub>50</sub> (nM)	JAK3 <sup>a</sup> IC <sub>50</sub> (nM)
<b>9</b>	-NH <sub>2</sub>	19	3,500
<b>10</b>	-NHCH <sub>3</sub>	10	1,600
<b>11</b>		64	3,400
<b>12</b>		50	5,400
<b>13</b>		70	3,600
<b>14</b>		50	8,600
<b>15</b>	-NH(CH <sub>3</sub> ) <sub>2</sub>	14,600	29,000

<sup>a</sup> Kinase activity was measured by Caliper assays, minimum in duplicate, average IC<sub>50</sub> reported.<sup>10</sup>

From this set of analogs, we were gratified to find that our design of compounds **9-14** (Table 2) resulted in a significant improvement in IRAK4 potency over the initial leads (**2, 8**, Table 1). As we had hypothesized amide **9** was a potent inhibitor of IRAK4. It appears that the C-2 substituent contributed significantly to maintaining selectivity over JAK3. Amide substitutions (**10-14**) were well tolerated in IRAK4, although increasing the size of the alkyl group on the amide (**11-14**) resulted in a modest decrease in IRAK4 potency compared to **10**. Finally, as anticipated from our examination of the IRAK4 crystal structure (Figure 1), the dimethyl analog **15** showed a significant loss in IRAK4 potency, presumably due to the loss of a hydrogen bond interaction with the amide carbonyl of Met265, or alternatively due to steric clash with the IRAK4 hinge region or a combination of both effects.

We were able to obtain an X-ray crystal structure of **10** bound to IRAK4 (Figure 3) which confirmed the binding mode observed in Figure 2. Comparing the crystal structures of **4** and **9** suggested that the bicyclic rings at C2 may be involved in a  $\pi$  stacking interaction with the gatekeeper residue (Tyr262). Additionally, a water molecule was observed that appeared to interact with the ligand as well as with Lys213, Glu233 or Asp329. Furthermore, it was noted that the hydroxyl on the phenylpropanol moiety at C4 may be involved in a hydrogen bond with Asp272.

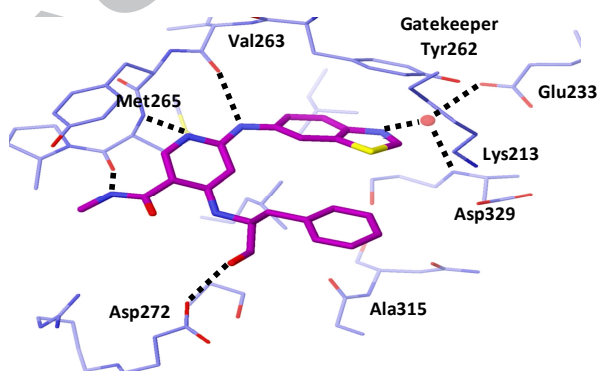
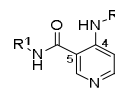


**Figure 3:** Crystal structure of **10** in IRAK4 kinase domain. Residues possibly involved in hydrogen bonds are labeled and bonds are shown by dotted lines. (PDB code 5W85).

With these positive initial results in hand, we turned our attention toward the exploration of the SAR at C4 while maintaining the benzothiazole group at C2 and the methyl amide at C5.

**Table 3.** SAR studies at C4.



Compound	R	R <sup>1</sup>	IRAK4 IC <sub>50</sub> (nM)	JAK3/ IRAK4 ratio
<b>16</b>	Me	Me	730	>50
<b>17</b>		Me	13	430
<b>18</b>		Me	20	300
<b>19</b>		Me	47	200
<b>20</b>		Me	130	100
<b>21</b>		Me	82	86
<b>22</b>		Me	170	200
<b>23</b>		Me	40	200
<b>24</b>		Me	25	200
<b>25</b>		Me	11	488
<b>26</b>		Me	21	800
<b>27</b>		Me	2,000	12
<b>28</b>		Me	50	230
<b>29</b>		Me	5	1400
<b>30</b>		H	20	1

<sup>a</sup> Kinase activity was measured by Caliper assays, minimum in duplicate, average reported.<sup>10</sup>

As indicated in Table 3, incorporation of a simple methyl group at C4 (**16**) resulted in a significant decrease in potency. In contrast, cyclopentyl and cyclohexyl groups (**17, 18**) improved potency over benzyl substitution (**17, 18** vs **8**). We had

anticipated that introduction of an alcohol group on the cyclohexane would improve both potency and selectivity by engaging in an interaction with Asp272. However, among the various stereo- and regio- isomeric cyclohexyl alcohols (**19-21**, **23-25**) or simple alkyl alcohols (**22**, **28**) that were prepared, no significant improvement in potency was observed, however introduction of a diol group on the benzyl amine moiety (**29**) did provide a modest improvement in potency. It is interesting to note the significant decrease in JAK selectivity between the alcohol **9** and diol **30**. This highlights the contribution of a secondary amide at this position to improved selectivity over JAK3.

With the exception of **29**, all of the compounds in Table 3 showed acceptable permeability (>150) in the parallel artificial

membrane permeability assay (PAMPA), but exhibited poor cellular potency (>1500 nM). The cause for this apparent disconnect is unknown. To probe this anomaly and as part of an effort to identify compounds with improved cellular activity and acceptable metabolic stability, SAR studies were conducted at C2 in combination with the methyl amide at C5 and the optimized diol group at C4. Groups at C2 were chosen such that we could study the effect of varying cLogP, number of hydrogen bond donors, groups known to block metabolic hotspots and improve solubility.

**Table 4.** SAR at C2.



Compound	R	IRAK4 <sup>a</sup> IC <sub>50</sub> (nM)	LTA_IL6 PBMc <sup>b</sup> IC <sub>50</sub> (nM)	PAMPA (nm/sec) @ pH 7.4	HLM % remaining <sup>c</sup>	MsLM % remaining <sup>c</sup>
<b>29</b>		5	300	19	90	21
<b>31</b>		5	1800	6	45	99
<b>32</b>		10	690	6	91	69
<b>33</b>		4	1600	6.5	59	42
<b>34</b>		13	5000	11	72	15
<b>35</b>		5	4100	51	98	73
<b>36</b>		10	1300	111	83	36
<b>37</b>		10	1600	70	65	41
<b>38</b>		13	3000	63	80	20

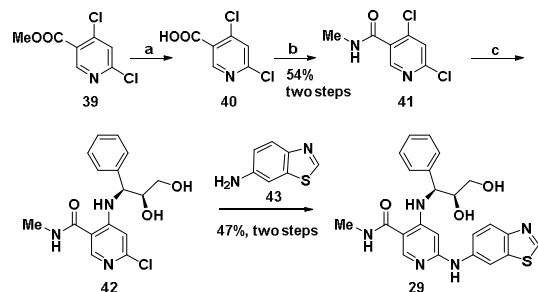
<sup>a</sup>Kinase activity was measured by Caliper assay. <sup>b</sup>LTA-IL6 assay. <sup>c</sup>Human and mouse liver microsome assay. All assays were done at a minimum in duplicate, average reported.

As depicted in Table 4, all of the compounds (**29-38**) were potent inhibitors of IRAK4, although none exhibited improved cellular potency as compared to **29**. All of the compounds also exhibited poor permeability (PAMPA < 150). Despite the poor permeability for compound **29**, upon further testing, it showed acceptable potency in a lipoteichoic acid (LTA) stimulated cellular assay in which inhibition of IL6 cytokine generation was measured (**30-38** were all > 1 μM).<sup>10</sup> In a human whole blood (LTA-IL6) assay<sup>10</sup> **29** also exhibited good potency (IC<sub>50</sub> = 300 nM). Furthermore, **29** was greater than 50-fold selective when tested against an in house set of kinases using a caliper assay, with the exception of LCK and MAP4K1 (HIPK1). In addition to

LCK and HIPK1, kinome wide screening (KINOMEScan®) revealed potent binding (< 10% of control) against DDR1, DDR2, FLT3, FLT1, MUSK, MER, RIOK2, TRKA, TRKB, and TIE1. In general, most of the compounds in this series showed acceptable stability in a human liver microsomal assay. However, due to poor murine metabolic stability (31% remaining after 10 min incubation), compound **29** was not progressed into mouse PK studies.

Synthesis of **29** is shown in Scheme 1. Methyl 4,6-dichloronicotinate (**39**) was hydrolyzed with LiOH in a 2:1 mixture of ethanol/water to afford acid **40**.<sup>10</sup> Acid **40** was converted to the corresponding acid chloride using oxalyl

chloride in the presence of catalytic DMF, and this mixture was then treated with methylamine to obtain methyl amide 4,6-dichloro-N-methylnicotinamide (**41**). Next, a solution of **41** was heated in the presence of (2S,3S)-3-amino-3-phenylpropane-1,2-diol and diisopropylethylamine (DIPEA) at 120 °C for 3 hours to obtain diol **42**. Finally, 6-aminobenzothiazole (**43**) and compound **42** were heated together in a sealed tube for 2 hours to obtain **29**.



**Scheme 1.** a) LiOH, EtOH/H<sub>2</sub>O (2:1), 22 °C, 4 h; b) Oxalyl chloride, DMF followed by methyl amine, 54% yield; c) (2S,3S)-3-amino-3-phenylpropane-1,2-diol, DIPEA, 120 °C, 3 h; d) 6-aminobenzothiazole, 1.2 equiv., 150 °C, 2 h, 47% yield.

## References and notes

- Navegantes, K. C.; de Souza Gomes, R.; Aparecida Tartari Pereira, P.; Czaikowski, P. G.; Heitmann Mares Azevedo, C.; Chagas Monteiro, M. J. *Transl. Med.* **2017**, *15*, 36.
- Kawai, T.; Akira, S.; *Nat. Immunol.* **2010**, *11*, 373.
- Sims, J. E.; Smith, D. E.; *Nat. Rev. Immunol.* **2010**, *10*, 89.
- Ku, C-L.; Bernuth, H.; Picard, C.; Zhang, S-Y.; Chang, H-H.; Yang, K.; Chrabieh, M.; Issekutz, A. C.; Cunningham, C.K.; Gallin, J.; Holland, S.M.; Roifman, C.; Ehl, S.; Smart, J.; Tang, M.; Barrat, F. J.; Levy, O.; McDonald, D.; Day-Good, N.K.; Miller, R.; Takada, H.; Hara, H.; Al-Hajjar, S.; Al-Ghonaïm, A.; Speert, D.; Sanlaville, D.; Li, X.; Geissmann, F.; Vivier, E.; Maródi, L.; Garty, B-Z.; Chapel, H.; Rodriguez-Gallego, C.; Bossuyt, X.; Abel, L.; Puel, A.; Casanova, J-L.; *J. Exp. Med.* **2007**, *204*, 2407.
- Picard, C.; Casanova, J-L.; Puel, A. *Clin. Microbiol. Rev.* **2011**, *24*, 490.
- Seganish, W. M.; *Ex. Op. Ther. Patents* **2016**, 26, 917.
- Chaudhary, D.; Robinson, S.; Romero, D. L.; *J. Med. Chem.*, **2015**, *58*, 96.
- Koziczak-Holbro, M.; Littlewood-Evans, A.; Pollinger, B.; Kovarik, J.; Dawson, J.; Zenke, G.; Burkhart C.; Müller, M.; Gram, H.; *Arthr. Rheumat.*, **2009**, *60*, 661.
- a) Lee, K.; Allais, C.; Ambler, C.; Anderson, D.; Boscoe, B.; Bree, A.; Brodfuehrer, J.; Bunnage, M.; Choi, C.; Chung, S.; Curran, K.; Day, J.; Dehnhardt, C.; Dermenci, A.; Drozda, S.; Frisbie,.; Gavrin, L.; Goldberg, J.; Han, S.; Hegen, M.; Hepworth, D.; Jacobson, B.; Kilty, I.; Kortum, S.; Lee, A.; Lovering, F.; Lowe, M.; Mathias, J.; Murphy, E.; Papaioannou, N.; Patny, A.; Pierce, B.; Ramsey, S.; Rao, V.; Saiah, E.; Shin, J.; Soutter, H.; Strobbach, J.; Symanowicz, P.; Thaisrivongs, S.; Thomason, J.; Trzuppek, J.; Vargas, R.; Vincent, F.; Wang, X.; Winkler, A.; Wright, S.; Yan, J.; Zapf, C.; *MEDI-261 Abstracts of Papers, 251st ACS National Meeting & Exposition, San Diego, CA, U.S.*, March 13-17, **2016**. b) Lee, K. L.; Ambler, C. M.; Boscoe, B. P.; Bree, A. G.; Bodfuehrer, C.; Cvhang, J. S.; Choi, C.; Chung, S.; Curran, K. J.; Day, J. E.; Dehnhardt, C. M.; Dower, K.; Drozda, S. E.; Frisbie, R. K.; Gavrin, L. K.; Goldberg, J. A.; Han, S.; Hegen, M.; Helpworth, D.; Hope, H. R.; Kamtekar, S.; Kilty, I. C.; Lee, A.; Lin, L-L.; Lovering, F. E.; Lowe, M. D.; Mathias, J. P.; Morgan, H. M.; Murphy, E. A.; Papaioannaou, N.; Patny, A.; Pierce, B. S.; Rao, V. R.; Saiah, E.; Samardjiev, I. J.; Samas, B. M.; Shen, M.W. H.; Shin, J. H.; Soutter, H. H.; Strobbach, J. W.; Symanowicz, P. T.; Thomason, J. R.; Trzuppek, J. D.; Vargas, R.; Vincent, F.; Yan, J.; Zapf, C. W.; Wright, S. W. *J. Med Chem.* **2017**, *60*, 5521-5542.
- Bhide, R. S.; Duncia, J. V.; Hynes, J.; Nair, S. K.; Pitts, W. J.; Srikantha, R. K.; Gardner, D.S.; Murugesan, N.; Paidi, V. R.; Santella, J. B.; Sistla, R.; Wu, H.; US 2015/0274696 A1
- Compounds 4, 10, and 7 have been assigned PDB IDs 5W84, 5W85, and 5W86, respectively.
- Kuglstatter, A.; Villasenor, A. G.; Shaw, D.; Lee, S. W.; Tsing, S.; Niu, L.; Song, K. W.; Barnett, J. W.; Browner, M. F. *J. Immunol.*, **2007**, *178*, 2641.

In conclusion, we have discovered a novel series of potent and selective IRAK4 inhibitors. This effort was aided by X-ray crystallography studies which revealed that the compounds bind to IRAK4 in a 'flipped' binding mode relative to the binding mode observed in JAK3 crystal structures for compounds from the same series. Key interactions included a classic hinge binding motif, and an apparent  $\pi$ - $\pi$  stacking interaction of the C2 substituents with the unique tyrosine gatekeeper in IRAK4. Attempts to improve binding by targeting a hydrogen bond to the carboxylic acid of Asp272 were less productive. Further studies describing optimization of the cellular potency and ADME properties of compounds in this series will be the subject of future disclosures.

## Acknowledgement

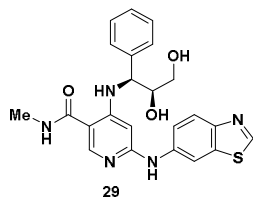
We would like to thank John Hynes for reviewing the manuscript. Also, we wish to thank the MDT team at Bristol-Myers Squibb, Dianlin Xie for the baculovirus expression of IRAK4 protein, Susan Kiefer for the IRAK4 protein purification, and Daniel Camac for the co-crystallization of **4**, **10**. Lastly, we would like to thank Proteros Biosciences GmbH for the co-crystal structure of **7** with JAK3.

## Graphical Abstract

**Discovery and structure-based design of 4,6-diaminonicotinamides as potent and selective IRAK4 inhibitors**

Leave this area blank for abstract info.

Rajeev S. Bhide, Alec Keon, Carolyn Weigelt, John S. Sack, Robert J. Schmidt, Shuqun Lin, Hai-Yun Xiao, Steven H. Spergel, James Kempson, William J. Pitts, Julie Carman and Michael A. Poss



IRAK4  $IC_{50}$  = 5 nM  
hWB LTA IL6  $IC_{50}$  = 300 nM